Ordered Nanopattern Arrangement of Gold Nanoparticles on β-Sheet Peptide Templates through Nucleobase Pairing

Takayuki Nonoyama,[†] Masayoshi Tanaka,[†] Yoshihito Inai,[†] Masahiro Higuchi,[‡] and Takatoshi Kinoshita[†,*]

[†]Department of Frontier Materials and [‡]Department of Materials Science and Engineering, Graduate School of Engineering, Nagoya Institute of Technology, Gokiso-cho, Showa-ku, Nagoya, Aichi, 466-8555, Japan

ABSTRACT We have demonstrated a unique method for rational arrangement of gold (Au) nanoparticles on a β-sheet peptide template through nucleobase pairing. For the template, the 16-mer peptide **1** was synthesized, which is based on an alternating amphiphilic sequence of Asp-Leu. Here Leu at the sixth position is replaced by thymine-modified Lys, and a polyethylene glycol chain is introduced to the C-terminus. The surface of Au nanoparticles was modified with the complementary adenyl group. Peptide **1** formed a stable β-sheet monolayer at the air/water interface under an appropriate surface pressure. The monolayer film transferred onto a mica surface by the Langmuir–Blodgett method showed a linearly striped pattern with 6.1 nm average stripe width and 6 nm average interval between stripes, derived from β-sheet assembly. The adenine-bound Au nanoparticles were successfully immobilized on the thymine-bound template through a complementary adenine–thymine hydrogen bonding pair. Interestingly, linear assembly structures of the Au nanoparticles were observed, thus being successfully reproduced by the original striped pattern of the template of **1**. Our method might readily fabricate Au materials with our desirable 2D pattern through fine-tuning of β-sheet sequence and nucleobase position.

KEYWORDS: nanopattern arrangement · gold nanoparticles · β-sheet peptide · nucleobase · template

A key step in nanoscience and nanotechnology is indeed to achieve our desirable arrangements of organic or inorganic species at the nanoscale. In organic nanomaterials, molecular components can be assembled through specific molecular interactions such as covalent and hydrogen bonds.[1,2] Such *directional* and *site-specific* interactions in intra- and intermolecules enable us to design and create elaborate hierarchical nanoarchitectures, as exemplified in proteins and cells. In contrast, the tailor-made arrangement of inorganic species is hardly controllable, because their attractive forces are based on *less directional* ionic and metallic interactions.

A variety of methods and techniques for fabricating a rational nanostructure of metallic particles have been attempted.[3−12] In particular, gold (Au)-based nanomaterials have been widely applied to functional devices such as electronic devices,[3] electron transistors,[4] catalytic potentials,[5] and sensors.[6] The versatile functionality originates from not only the metallic nature of Au itself but also the spatial arrangement of Au particles. For instance, multilayer thin films consisting of self-assembled Au nanoparticles are created on a mercapto-modified surface through treatment with dithiol and subsequent immersion in an Au solution.[3] The resultant thin films provide unique nonmetallic electronic and optical properties. As another example, Au colloidal nanoparticles are organically linked together through treatment with dithiol.[4] The Au particle chain can be used as a "bridge" for a single electron transistor with a multitunnel junction structure. A monolayer of biotin-coated Au nanoparticles on a glass surface constitutes a highly sensitive biosensor.[6] A topologically patterned Au or Ag–Au array was also obtained from Au nanoparticles on a poly(dimethylsiloxane) stamp through nanotransfer printing or nanotransfer edge printing technique.[7]

Despite these elegant approaches, there is still a gap between inorganic and organic (or biological) matters in the control of nanospacing. Thus the fabrication of rational inorganic array structures is addressed as one of the most challenging fields in nanoscience. To diminish the gap, it has been proposed that biological templates are an effective tool for fabricating a position-specific inorganic array structure.[10−12] For instance, β-sheet-forming oligopeptides, which preferentially bind to Au surfaces, are self-assembled in Au buffer solutions, simultaneously generating unique Au-nanoparticle double helices along the peptide template.[10,11] The Au-superstructural features can also be tuned with various synthetic conditions.[11] Another unique example of using a peptide template is the combinatorial phage–display library method.[12] It enables one to select a peptide-specific inorganic compound to build up its directional nanocrystal assembly.

* Address correspondence to kinoshita.takatoshi@nitech.ac.jp.

Received for review February 22, 2011 and accepted July 8, 2011.

Published online July 08, 2011
10.1021/nn200711x

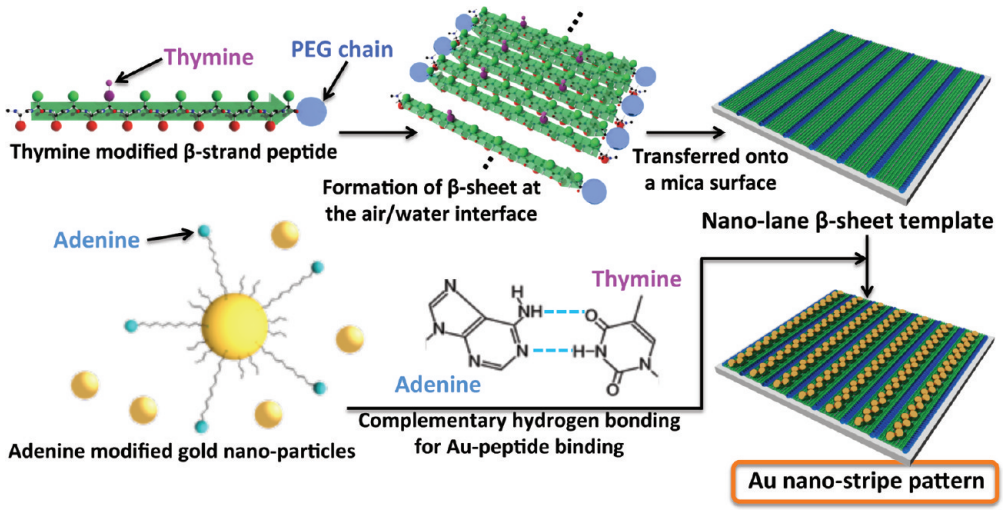

Figure 1. Our method for fabricating a unique 2D assembly pattern of Au nanomaterials on a β-sheet monolayer template through nucleobase pairing.

We here propose another unique approach to a peptide template-specific assembly of Au nanoparticles. As a key for the Au–peptide binding, complementary nucleobase pairs have been chosen. Nucleobase pairing based on multivalent hydrogen bonds has commonly been recognized as highly site-specific interactions for creating DNA and supramolecular assemblies.[13–15]

The outline of our present method is illustrated in Figure 1. First, an amphiphilic β-sheet peptide is chosen for the peptide template. Herein a single nucleobase group (thymine) is covalently introduced to a hydrophobic face of the amphiphilic sequence. The peptide at the air/water interface is aggregated to form a β-sheet monolayer, which is then transferred onto a mica substrate by the vertical dipping method with upstroke. Second, Au nanoparticles are chemically modified with the complementary nucleobase groups (adenine) through formation of an Au–sulfide bond. Addition of the modified Au particles gives rise to spontaneous nucleobase pairing at thymine groups on the β-sheet template. Consequently, a unique two-dimensional (2D) assembly structure of Au nanoparticles can be rationally controlled by a 2D nucleobase pattern drawn on the β-sheet template. The benefit of our method is that another 2D nucleobase pattern is easily prepared through the variation of the amino acid sequence for structurally well-defined β-sheets.

To demonstrate our method, we employed the 16-mer peptide **1** for the β-sheet template.

$$\mathrm{Ac-(Asp-Leu)_2-[Asp-Lys(Thy)_{\mathit{x}}(Ac)_{1-\mathit{x}}]-(Asp-Leu)_5-PEG_{70}}\quad \mathbf{1}$$

[Ac, acetyl; Lys(Thy), Lys of thyminyl-capped N^{ε}-amino group; PEG_{70}, polyethylene glycol having 70 ethylene glycol (EG) units; $x \approx 0.36$].

Peptide **1** is based on a sequential alternating amphiphilic sequence (Asp-Leu) for adopting a β-sheet. The sixth hydrophobic position is replaced by Lys, whose N^{ε}-amino group is capped with the thymine moiety. A PEG chain is attached to the C-terminal position to enhance its hydrophilicity. The C-terminal PEG is also expected to maintain a constant distance between β-sheet fibers and to prevent unfavorable amyloid-like aggregations.[16] As a result, peptide **1** at the air/water interface took a stable β-sheet to yield a thymine-bound monolayer template. Adenine-modified Au nanoparticles were immobilized on the thymine-bound template through complementary nucleobase hydrogen bonding. Linear assembly structures of the Au nanoparticles were successfully obtained, thus being reproduced by the original stripe pattern of the template.

RESULTS AND DISCUSSION

Design of an Amphiphilic Peptide Having a Thyminyl Moiety for a Template. Peptide **1** (Chart 1) is designed with an amphiphilic oligopeptide and a PEG chain. The peptide part is a 16-mer of alternating amphiphilic sequence based on Asp-Leu. Herein the sixth hydrophobic position from the N-terminus is replaced by Lys having a thyminyl group in the side chain. We dared not to place the modified Lys at around the center of the 16-mer sequence. The central position would disturb the dense arrangement of Au nanoparticles, because thyminyl–thyminyl pairs on two neighboring chains packed into a β-sheet are close to each other. In the case of noncentral positions, such unfavorable proximity would still occur on a parallel β-sheet, but not prominently on an antiparallel β-sheet. Peptide **1** should favor an antiparallel β-sheet similar to another amphiphilic peptide.[17–19] Thus the modified Lys residues on an antiparallel β-sheet face should be arranged in a zigzag pattern, exchanging between the sixth and 11th positions, thereby relaxing the steric hindrance of the Au nanoparticles bound to two neighboring chains. In addition, the fraction of thyminyl group incorporated was shown to be about 36%. The functionality of *ca.*

Chart 1. (a) Amphiphilic β-sheet peptide 1 and (b) its molecular size.

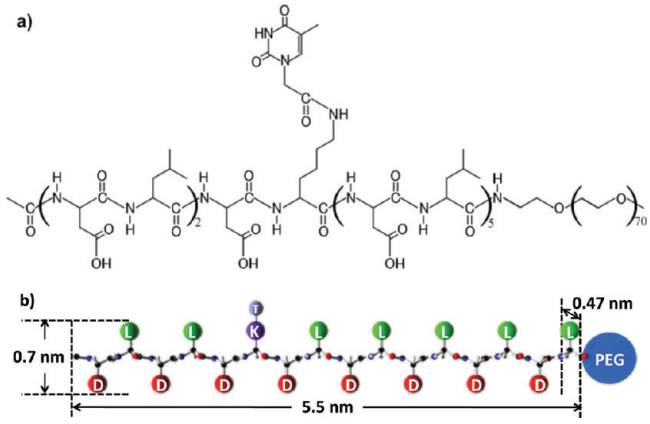

1/3 should further moderate a dense arrangement of Au nanoparticles.

Oligopeptides with such an alternating amphiphilic sequence, at the air/water interface, facilitate forming a β-strand structure,[20] because all hydrophilic side chains on the same face are spontaneously directed toward the water phase. Also in peptide **1**, each carboxyl group of Asp is preferentially located in water. Conversely, the hydrophobic alkyl chain of Leu and the thyminyl group of Lys are directed to the air phase.

The C-terminal PEG chain is expected to act as a spacer between two neighboring β-sheet lanes. Our previous work[20] revealed that similar amphiphilic β-sheet peptides without a PEG chain are readily aggregated to form an amyloid-like fiber. The incorporated PEG chain, thus, should prevent unfavorable peptide aggregation, thereby facilitating the formation of a 2D β-sheet monolayer.

Fabrication and Structural Analysis of the Template. We fabricated a template composed of thymine-modified amphiphilic peptide **1** by the standard Langmuir–Blodgett (LB) technique (for the detailed procedure, see the Experimental Section). Figure 2 shows the surface pressure–area (π–A) isotherm of peptide **1** in the water phase at pH 2.8, where the area is expressed per molecule **1**. A standard π–A profile was obtained here. That is, the π value gradually increases with decreasing area, then drastically increased in the area below 5–6 nm^2. Thus the whole π–A curve is approximately expressed with two lines of gentle and steep slopes. Extrapolation of the steep line to π = 0 yielded the limiting area per molecule **1**, 5.68 nm^2 (indicated by the arrow in Figure 2). This value was somewhat smaller than the calculated value of 6.89 nm^2, in which the area of the PEG_{70} chain was estimated to be 4.30 nm^2 from the freely jointed chain model, and that of the peptide domain was 2.59 nm^2. The reason for this is that the highly hydrophilic PEG chain might be partly sunk down into the aqueous phase under a higher surface pressure. As a result, the calculated PEG area is overestimated.

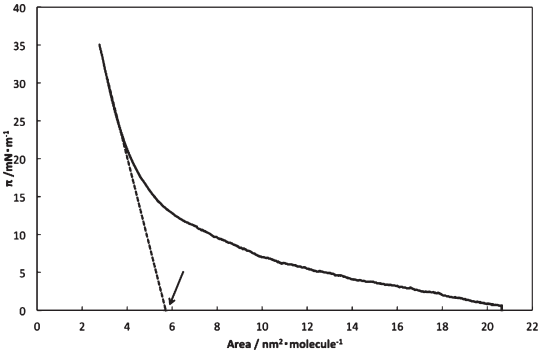

Figure 2. π–A isotherm of peptide 1 in the aqueous solution at pH = 2.8 at 25 °C. The arrow indicates the limiting area per molecule.

Figure 3 displays atomic force microscope (AFM) images of the corresponding **1**'s LB films prepared under a surface pressure of 10, 15, or 20 mN/m. While all the morphologies showed a fiber-like pattern, their fiber lengths depended largely on the surface pressure. A low surface pressure (10 mN/m) gave considerably short fibers, having a 7.1 nm average length on the AFM image. A fiber pattern was clearly seen at a middle pressure (15 mN/m). A high pressure (20 mN/m) yielded a nanostripe pattern assembled by long fibers. Each stripe was characterized by a 0.6 nm average height and a 12 nm average width on the AFM image. In general, AFM analysis overestimates the sample width depending on the shape of the scanning tip. According to Fung's equation for AFM-derived width calibration,[21] the corrected width of the nanostripe pattern was estimated to be 6.1 nm. This value is consistent with the calculated molecular length (5.5 nm) for the peptide part adopting a β-sheet conformation.

The conformation of peptide **1**'s LB film (10 layers) prepared at a surface pressure of 20 mN/m was investigated by circular dichroism (CD) and transmittance Fourier transform infrared (TM-FTIR) measurements. The CD spectrum (Figure 4a) showed a convex profile with a negative minimum at around 215 nm, typical of a β-sheet conformation.[22] The amide I region in the

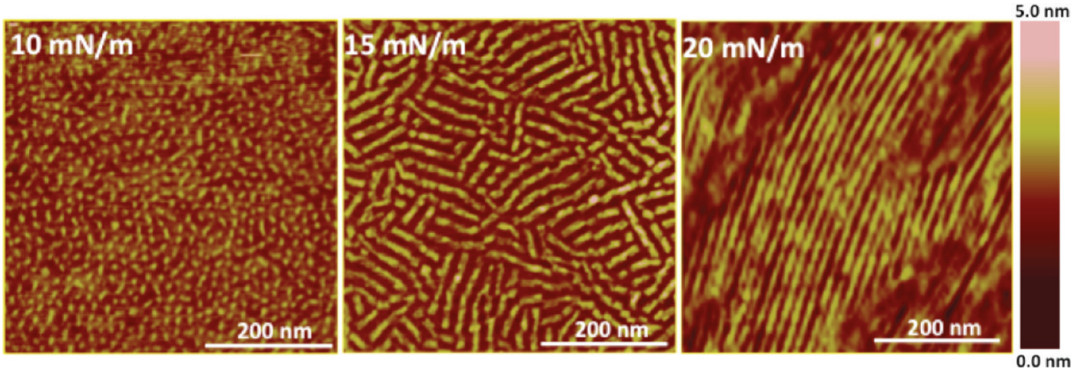

Figure 3. AFM images of the monolayers of 1 transferred onto a mica plate. The transfer process was performed by the vertical dipping method on upstroke at a surface pressure of 10, 15, or 20 mN/m.

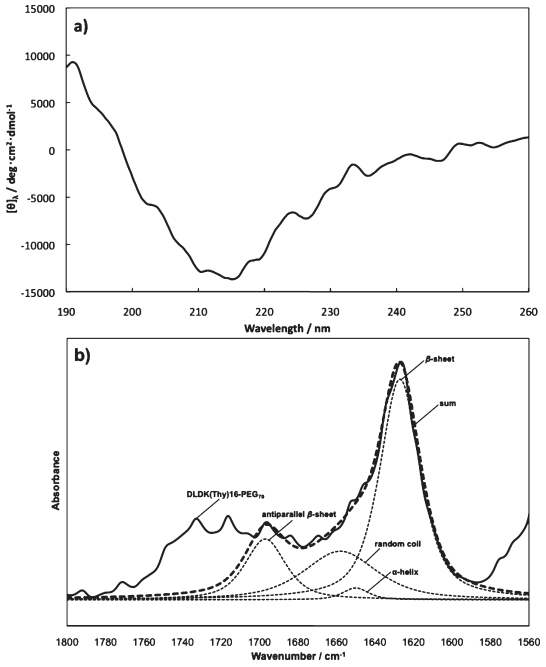

Figure 4. (a) CD and (b) TM-FTIR spectra of 1's LB film onto a CaF_2 plate. The transfers were performed 10 times by the vertical dipping method on up- and downstrokes at 20 mN/m. (b) Broken lines show the peak deconvolution of the amide I band to β-sheet, α-helix, random coil, and antiparallel β-sheet conformation.

TM-FTIR spectrum (Figure 4b) consisted of a major absorption band at around 1630 cm^{-1} and some minor bands at 1700−1640 cm^{-1}. Two bands of around 1690 and 1630 cm^{-1} suggest the presence of an antiparallel β-sheet.[23,24] The fractions of antiparallel β-sheet, α-helix, and random coil[23−26] were estimated, from curve fitting of the observed spectrum, to be 75% β-sheet, 2% α-helix, and 23% random coil. These CD and TM-FTIR results reveal that the nanostripe film is comprised primarily of antiparallel β-sheet chains.

The surface pressure-induced morphological changes could be explained as follows. Under a lower surface pressure, the PEG part of **1** on the water surface should favor an expanded form, which might disturb the growth of β-sheet chains into large fibers. In contrast, a higher pressure increases the surface concentration of **1** to facilitate the formation of longer β-sheet fibers. At this point the PEG chain bound to the peptide C-terminus can act as a spacer or a cushion between the β-sheet fibers, thus disturbing excessive, unfavorable self-aggregation (leading to amyloid-like or random aggregates) even at higher pressure condition. As a result, the combination of the C-terminal PEG and a higher surface pressure facilitates the formation of the β-sheet-based nanostripe pattern with a regular interval (6 nm average distance between neighboring stripes).

Characterization of Adenine-Modified Au Nanoparticles. The preceding nanostripe film was employed for the thymine-modified template. In turn, Au nanoparticles as an inorganic target were modified with the complementary adenyl group. The diameter of the nanoparticles must be less than the nanostripe width (6.1 nm) and the space between neighboring β-strand chains (4.65 nm). Here Au nanoparticles with a small diameter, ca. 1 nm, were prepared. Such a particle size was controlled with feed ratios of hydrogen tetrachloroaurate(III) ($HAuCl_4$) to the thiol groups of 1-propanethiol (C_3) and 11-mercapto-1-undecanol ($C_{11}OH$).[27] A wine-red colloidal solution of adenine-modified Au nanoparticles [Au(Ade)NPs] in chloroform originates from a small absorption band at 500 nm (Figure 5a). This band is assigned to the plasmon band of Au nanoparticles, thus supporting successful synthesis of adenine-coated Au nanoparticles. The adenyl amount per particle was also determined to be 0.68 mmol/g from absorbance at 264 nm of the colloidal solution by using the molar extinction coefficient of adenosine.[28]

The size of Au(Ade)NPs was estimated from the AFM image. As shown in Figure 5b, the nanoparticles were homogeneously dispersed on a mica surface. The average diameter was estimated to be 1.1 nm from the height of each particle in the cross section. We calculated the number of adenyl groups per Au nanoparticle using eq 1:[29]

$$\frac{1}{6}d^3\rho n\pi N_A \times 10^{-21}\ \text{molecules/particle} \qquad (1)$$

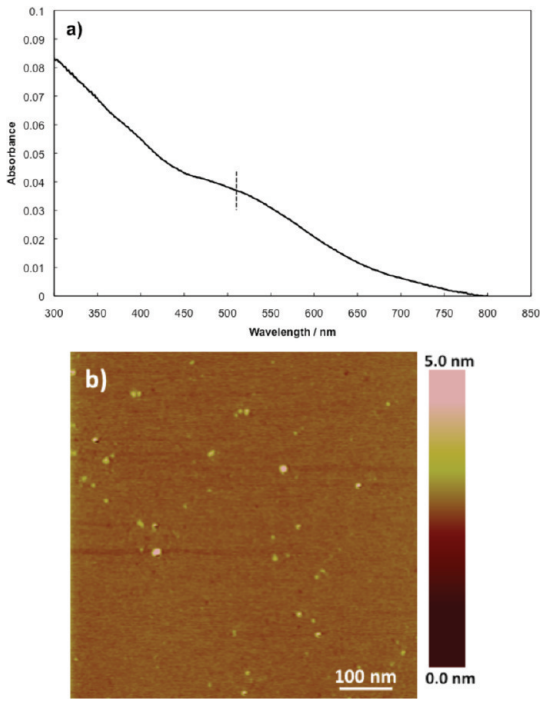

Figure 5. (a) UV/vis spectrum of Au(Ade)NPs in chloroform. The concentration of the nanoparticles was adjusted to 1.0 × 10^{-2} mg/mL. (b) AFM image of Au(Ade)NPs in chloroform. An aliquot of a colloidal solution of Au(Ade)NPs in chloroform (2.2 × 10^{-2} mg/mL) was placed on freshly cleaned mica, allowing the nanoparticles to be adsorbed on its surface. After the absorption, the excess solution was removed by absorption onto filter paper.

where d is the diameter of Au(Ade)NPs in the AFM measurement (1.1 nm); ρ, the density of gold (19.3 g/cm^3); and n, the amount of adenyl group on the particle surface (0.68 mmol/g). As a result, 5.5 adenine groups were introduced into a single nanoparticle. Au(Ade)NPs obtained here were characterized by a very small particle size and a sufficient number of adenyl groups, thus being expected to sit on the thyminyl groups of the template.

Ordered Nanopattern of the Au Nanoparticles on the Peptide Template. For our purpose, we have attempted to fabricate an ordered nanostructure of the Au(Ade)NPs on the monolayer template. As seen in Figure 2, the template alone, prepared at a surface of 20 mN/m, shows a regular nanostripe pattern. The peptide template was immersed into a suspension of Au(Ade)NPs in chloroform (2.2 × 10^{-2} mg/mL) at 20 °C. After being incubated at 20 °C for 1 h, the template was rinsed with pure chloroform several times. AFM images of the resultant template are shown in Figure 6a. Au nanoparticles appear to be immobilized on the original nanostripe pattern. From a cross section analysis, the average height of the particles was 1.8 nm from the bottom surface of mica. This value is in good agreement with summation of the height of the peptide template (0.6 nm) and the diameter of the Au particle (1.1 nm). Thus the original template structure is not destructed by immobilization of the nanoparticles.

Figure 6b shows an AFM image of the template prepared through another incubation at a higher temperature (40 °C for 1 h). Interestingly, the nanoparticles on the template dramatically decreased, compared to the incubation at 20 °C (Figure 6a). Thus the temperature-sensitive immobilization supports the view that Au nanoparticles bind to the template through complementary hydrogen bonding of thymine−adenine pairs. Such multivalent hydrogen bonds, due to an exothermic process, weaken at a higher temperature. In fact, thymine−adenine hydrogen bonds were broken at 30−35 °C or above in variable-temperature NMR experiments using model compounds in solution (for details, see Figure S1).[30−32]

To shed light on the nucleobase-pairing effect on the immobilization, Au nanoparticles modified with C_3 and $C_{11}OH$, Au(C_3)NPs were prepared. Au(C_3)NPs were used instead of Au(Ade)NPs. The Au(C_3)NP template was prepared through incubation at 20 °C as mentioned above. The AFM image (Figure 7a) indicates that no Au(C_3)NPs particles are essentially found on the peptide template. Moreover, we investigated the combination of Au(Ade)NPs with another peptide, **2**, lacking the thyminyl group in peptide **1**: **2**, Ac-(Asp-Leu)$_2$-[Asp-Lys(Ac)]-(Asp-Leu)$_5$-PEG$_{70}$; Lys(Ac), N$^{\varepsilon}$-acetyl Lys. The Au(Ade)NP template of **2** was also prepared through incubation at 20 °C. The AFM image (Figure 7b) reveals that Au(Ade)NPs are not absorbed on the template of **2**, whereas the template itself also shows a nanostripe pattern. Therefore, successful immobilization of Au(Ade)-NPs on the template of **1** (Figure 6) is unambiguously derived from the complementary nucleobase pairing. Accordingly, the Au particles should be rationally put on thyminyl positions preorganized on the β-sheet surface.

Figure 8a shows the AFM image of Au(Ade)NPs immobilized on the template of **1**. The incubation for adsorption of the nanoparticles was carried out at 20 °C for 24 h. In comparison with the incubation at 1 h (Figure 6a), the surface density of the nanoparticles was greatly increased by the prolonged incubation period. More interestingly, linear assembly structures of the nanoparticles were clearly observed here, which appears to reflect the original stripe pattern of the template **1** alone (Figure 8b).

For a more quantitative evaluation, the order parameter P_2 for linear arrangements of the nanoparticles was calculated from 2D fast Fourier transform (2D-FFT) of the AFM image (Figure 8a) to be −0.26: for the definition of P_2, see the Experimental Section. On the other hand, Au(Ade)NPs alone on mica form large aggregates (Figure 8c), whose the P_2 value was −0.09. It should be noted that the P_2 parameter ranging from 0 to −0.5 takes a larger negative value when objects of interest are more highly ordered. It is obvious that the template of **1** promotes the ordered state of Au(Ade)NPs. Furthermore, the P_2 value for a nanostripe pattern of the template of **1** alone was estimated to be −0.27 (Figure 7b). Interestingly, this value is approximately

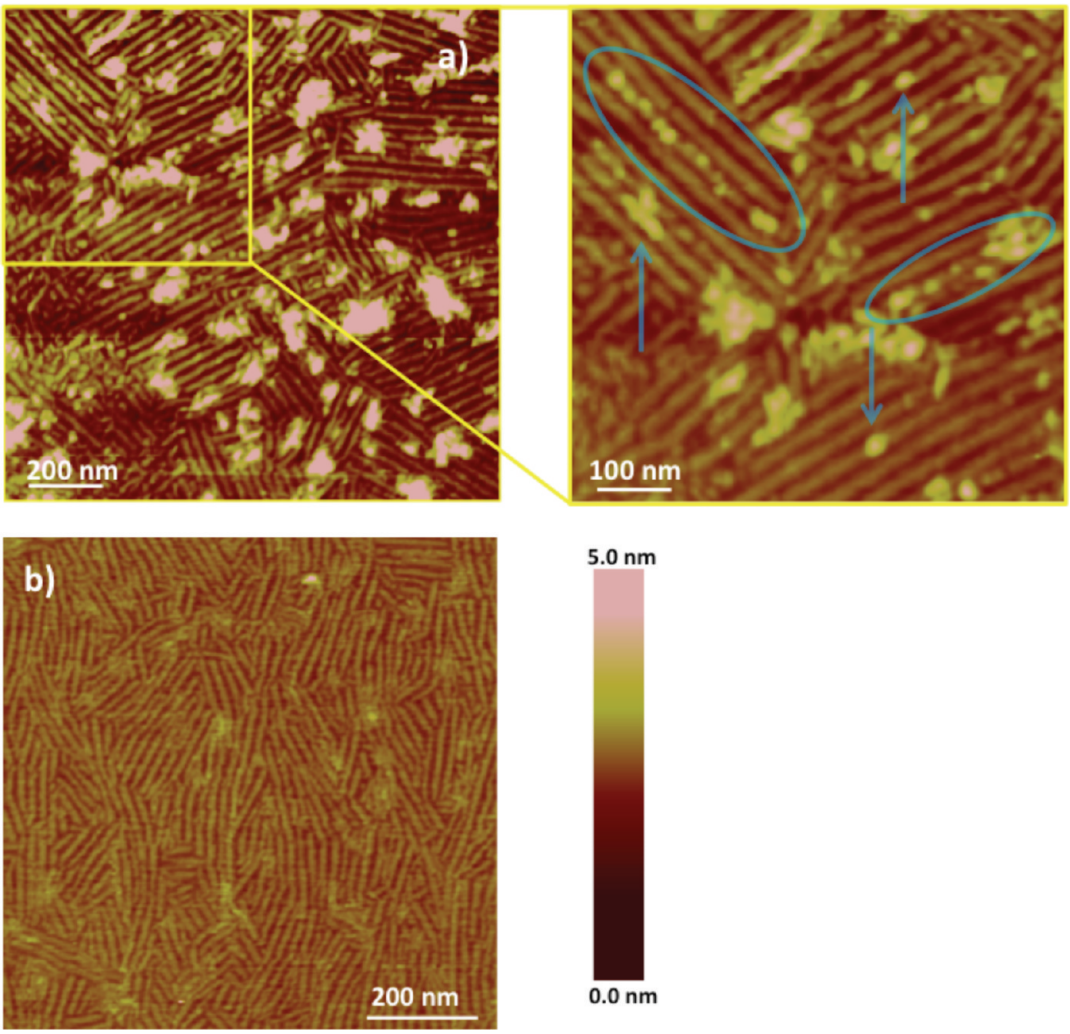

Figure 6. AFM images of adsorbed Au(Ade)NPs on the template of 1. The adsorption of the nanoparticles on the template was carried out for 1 h at (a) 20 °C and (b) 40 °C, respectively. The blue circle indicates that the Au nanoparticles were immobilized on a peptide nanofiber.

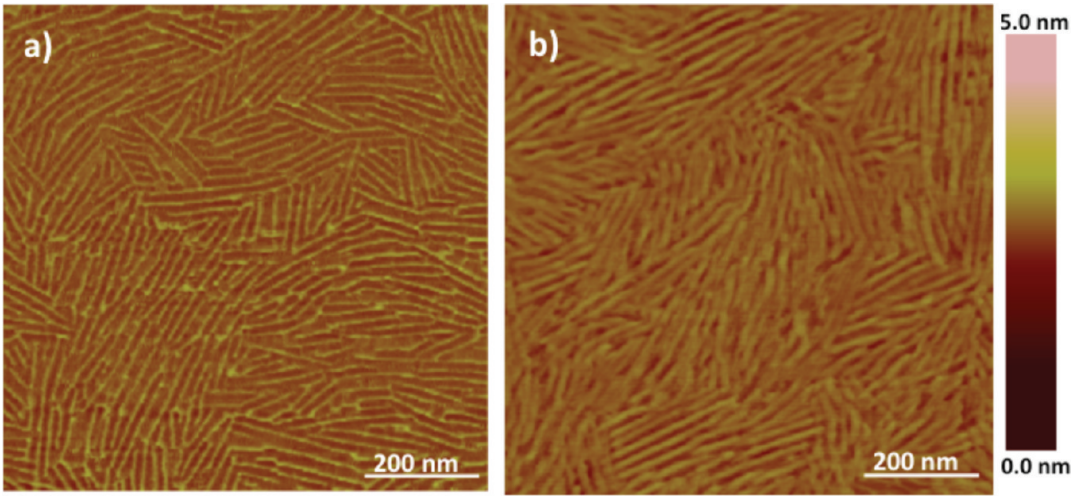

Figure 7. AFM images of (a) Au(C_3)NPs adsorbed on the template of 1 and (b) Au(Ade)NPs adsorbed on the template of 2 having no thymine group.

equal to −0.26 of the Au(Ade)NPs linearly assembled on the template (Figure 7a). The significant similarity of the two P_2 values strongly supports that the linear-assembled structures of Au(Ade)NPs are *reproduced* by

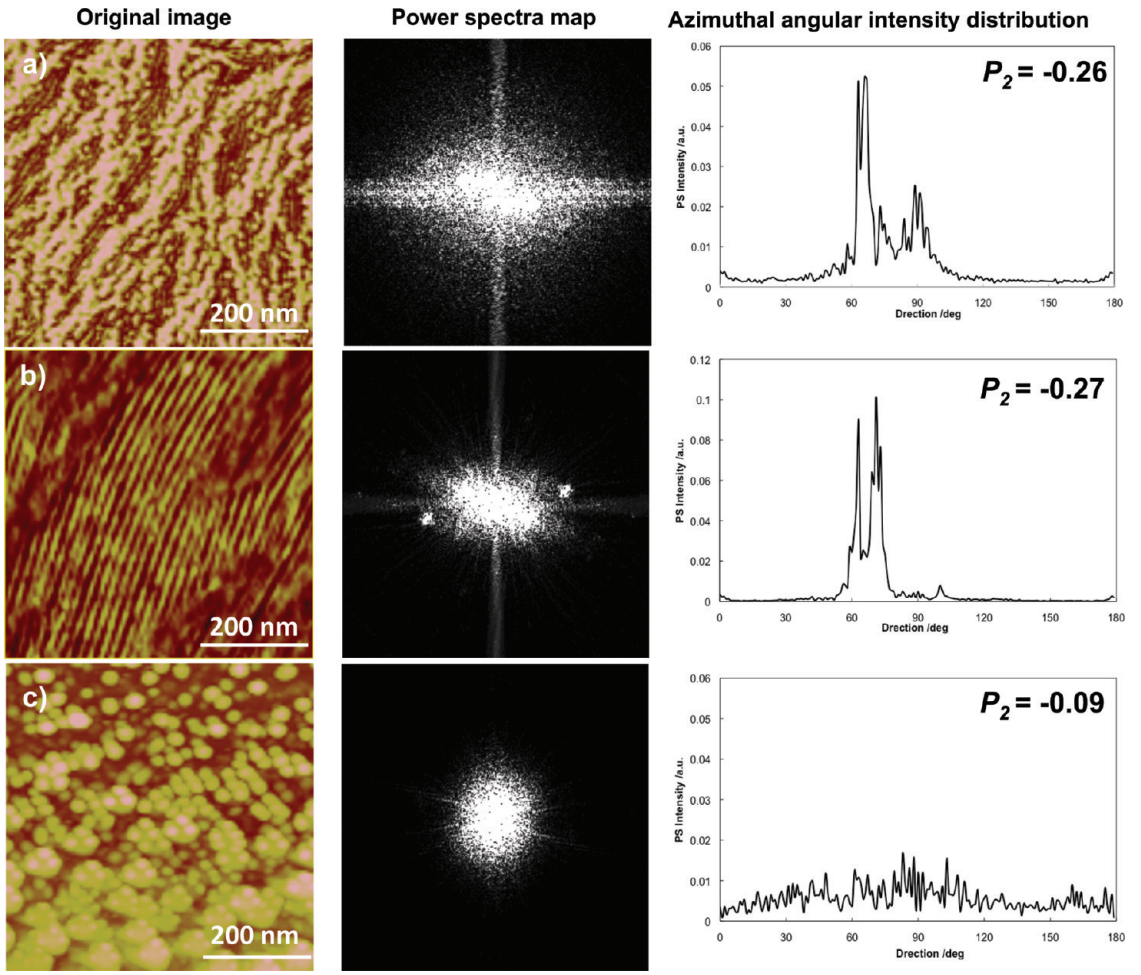

Figure 8. AFM images, their power spectral maps, and azimuthal angular intensity distributions: (a) Au(Ade)NPs assembled on the template of peptide 1, (b) template of 1 alone, and (c) Au(Ade)NPs adsorbed on a mica plate. The order parameter P_2, calculated from the azimuthal angular intensity distributions, is shown in the corresponding figures. Adsorption of the nanoparticles on the template of 1 or a mica plate was carried out at 20 °C for 24 h.

the thymine-bound stripe pattern through complementary nucleobase pairing.

CONCLUDING REMARKS

We here have demonstrated a rational assembly of inorganic nanoparticles on organic monolayers through directional site-specific interaction. The adenine-modified Au nanoparticles, although statistically distributed on a mica surface, can be regularly arranged on a β-sheet-striped surface that holds thyminyl groups in a position-specific 2D pattern. The nanoparticles are distributed on the thyminyl sites preorganized on the β-sheet template through complementary hydrogen bonding for adenine–thymine pairs. Consequently, linearly striped assembly structures of the Au nanoparticles are successfully fabricated in response to the nanostripe pattern of the thymine-bound template.

As the most striking feature of our method, we can readily design another β-sheet template tailoring our desired nucleobase pattern, because the β-sheet backbone is a well-defined structure. On the basis of β-sheet sequence design, standard solid-phase synthesis enables us to modify the original amino acid sequence to control the size of the β-sheet template or the thyminyl position. A variety of such templates offer the corresponding thyminyl 2D pattern to reproduce a unique Au-assembly structure. Our method would also control the assembly structures of two kinds of inorganic materials through simultaneous use of the other nucleobase pair, guanine–cytosine, as well as the thymine–adenine pair.

EXPERIMENTAL SECTION

Materials. PEG-loaded resin, commercially available from RAPP Polymers GmbH, was used as a starting material for solid-phase peptide synthesis. It contains an Fmoc-protected amino group at one terminal of the PEG chain: for a ratio of amino group incorporated of 0.24 mequiv/g and for an average

molecular weight of PEG chain of 3080 (number of EG repeating units, 70). Fmoc-amino acids (Fmoc, 9-fluorenylmethyloxycarbonyl) was also purchased: Fmoc-Leu-OH, Fmoc-Asp(O^{t}Bu)-OH (O^{t}Bu, *tert*-butyloxy) and Fmoc-Lys(Mtt)-OH [Lys(Mtt), N^{ε}-methyltrityl-lysine; Mtt, N$^{\varepsilon}$-methyltrityl].

Synthesis of Ac-[Asp(O^{t}Bu)-Leu]$_2$-[Asp-Lys(Mtt)]-[Asp(O^{t}Bu)-Leu]$_5$-PEG$_{70}$. Peptide **1**, protecting all side-chain functional groups, was synthesized by conventional solid-phase method[33] (see Figure S2). The detailed procedure is as follows.

The PEG-loaded resin (200 mg) was swollen in 5 mL of dichloromethane (DCM) for 1 day, then rinsed with 5 mL of dimethylformamide (DMF) three times. Prior to the first condensation, the Fmoc group was removed by treatment of a DMF solution containing 20 vol % piperidine. After 1 h, piperidine was removed by rinsing with DMF. To the resin/DMF mixture were added Fmoc-amino acid (0.12 mmol) in 3 mL of DMF, 1,3-diisopropylcarbodiimide (0.36 mmol) in 1 mL of DMF, and 1-hydroxy-7-azabenzotriazole (0.36 mmol) in 1 mL of DMF. The suspended mixture was shaken for 2 h to couple Fmoc-amino acid to the amino group in the resin. Then the resin was rinsed with DMF. Prior to the next condensation, the Fmoc group was removed in a similar manner to that mentioned above. The deprotected amino group was coupled with Fmoc-amino acid, as mentioned above. This deprotection−coupling process was successively repeated to reach the desired sequence.

In the final 16-mer sequence, the Fmoc group of N-terminal Asp(O^{t}Bu) was removed as mentioned above. The resultant N-terminal amino group was acetylated by treatment for 2 h with a pyridine solution (6 mL) containing 33 vol % acetic anhydride. The mixture was rinsed with DCM to obtain the resin possessing the 16-mer peptide.

Synthesis of Peptide 1. The thyminyl group was introduced into the side chain of Lys as follows. The Mtt group of Lys(Mtt) was removed with 5 mL of a DCM solution containing 2 vol % trifluoroacetic acid (TFA), 2 vol % triisopropylsilane, 4 vol % thioanisol, and 0.6 mL of water for 10 min.[34] After rinsing with DCM, thymine-1-acetic acid was coupled to the N$^{\varepsilon}$-amino group of Lys, according to a manner similar to coupling of Fmoc-amino acid in the preceding section. The coupling process was monitored by the 2,4,6-trinitrobenzenesulfonic acid test[35] and continued until the N$^{\varepsilon}$-amino group disappeared.

The 16-mer-bound resin was dried *in vacuo* and then stored in an ice bath. To the precooled resin was added a precooled aqueous solution (10 mL) containing 95 vol % TFA, 8.5% ethanedithiol, and 5 vol % thioanisol. The mixture stood for 1 h at room temperature to remove all O^{t}Bu groups of Asp residues and to detach the peptide-PEG polymer from the resin. After the remaining resin was filtered out, the filtrate was concentrated to a volume of ca. 1−2 mL under reduced pressure. After precooled diethyl ether (100 mL) was added, our final product **1** was recovered as precipitates. The product was checked by ^{1}H NMR spectroscopy (see Figure S3).

The proton integral ratio of (8H, Asp C$^{\alpha}$H):(8H, Leu and Lys C$^{\alpha}$H):(42H, Leu C$^{\delta}$H$_3$) was shown to be 7.9:8.1:42, indicating the successful solid-phase synthesis of the 16-mer peptide. On the other hand, the fraction of thyminyl group incorporated was estimated to be ca. 0.36, from the observed ratio of 0.37:0.34:42 for (1H, thyminyl NH):(1H, thyminyl vinyl H):(42H, Leu C$^{\delta}$H$_3$).

Preparation of Adenine-Modified Au Nanoparticles. A synthetic route of Au(Ade)NPs is illustrated in Figure S4. Au(C$_3$)NPs were prepared. Hydroxyl groups located on the surface of Au(C$_3$)NPs were used as reaction sites for incorporation of adenyl group. As shown in Figure S4, Au(C$_3$)NPs were prepared by reduction[36] of $HAuCl_4 \cdot 4H_2O$ with sodium borohydride ($NaBH_4$) in the presence of C$_3$ and C$_{11}$OH. The detailed procedure is as follows.

$HAuCl_4$ was dissolved in 1 L of pure water at $[HAuCl_4] = 2.0 \times 10^{-4}$ M. To the $HAuCl_4$ aqueous solution was slowly added an ethanol solution of C$_3$ and C$_{11}$OH (5 mL each) at [$HAuCl_4$]:[C$_{11}$OH]:[C$_3$] = 10:3:27. To the solution was added 10 mL of an ice-chilled aqueous solution of $NaBH_4$ (2 mM; 10 molar equiv for $HAuCl_4$) with vigorous stirring. After stirring at room temperature for 1 h, the mixture was concentrated to ca. 100 mL, and then the solution was dialyzed overnight against 1 L of distilled water using a Spectra/Pore molecular porous membrane tube (Spectrum Medical Industries, Inc., MWMC35-00). The remaining solution was lyophilized to obtain Au nanoparticles modified with hydroxyl groups on the surfaces of Au(C$_3$)NPs.

Au(Ade)NPs were obtained by coupling between adenine phosphoramidite and hydroxyl groups of Au(C$_3$)NPs,[37] as follows. Au(C$_3$)NPs (100 mg) were added to adenine phosphoramidite (1 g) dissolved in 5 mL of dry acetonitrile (AcCN). To the suspended mixture was added an AcCN solution of tetrazole (0.45 M) with vigorous stirring. After being stirred at room temperature for 2 h, the reaction mixture was diluted with 20 mL of pure water, and then the solution was lyophilized. After the remaining solution was dried, the resultant nanoparticles were suspended in a 0.02 M iodic aqueous solution containing tetrahydrofuran and pyridine, and the suspended mixture was stirred for 2 h to oxidize the phosphite to phosphate. After addition of 6 mL of purified water, the suspended mixture was dialyzed until iodine was completely removed. After lyophilization, the corresponding nanoparticles were obtained.

The nanoparticles were dispersed in 10 mL of AcCN solution containing 3 vol % of trichloroacetic acid (0.02 M), and the suspension was stirred for 2 h to remove the 4,4′-dimethoxytrityl protecting groups of the 5′-hydroxyl group of deoxyadenosine. After evaporation, the residue was stirred for 24 h with 5 mL of an aqueous solution containing 28 wt % ammonia and 5 mL of 1,4-dioxane to remove the benzyl protecting group of the adenine moiety and the β-cyanoethyl protecting group of phosphate moiety. After addition of pure water, the suspension was dialyzed overnight as mentioned above and then lyophilized to obtain adenine-modified Au nanoparticles. The crude product was purified through silica gel column chromatography using AcCN as eluent. The first elution fraction was collected and concentrated to ca. 10 mL, and then 90 mL of purified water was added. The suspension was lyophilized to obtain the final adenine-modified Au nanoparticles.

Measurements. *Surface Pressure−Area Isotherms.* π−A isotherms of peptides **1** and **2** monolayers were recorded on a Filgen NL-BI040-MWCT instrument by using a LB film balance. Milli-Q-treated water was used as the subphase, of which the pH was adjusted to 2.8 by addition of hydrogen chloride. Each peptide sample was dissolved in benzene at 0.1 mg/mL. A small amount of the peptide solution was delivered to the water surface with a microsyringe. The corresponding π−A isotherms at a compression rate of 5 mm/min were taken under the subphase at 25 °C.

Spectroscopic Measurements. UV/vis absorption spectra of Au(Ade)NPs and Au(C$_3$)NPs in chloroform were recorded on a Jasco V-550 spectrophotometer. The conditions are as follows: ambient temperature; optical path length, 10 mm; Au concentration, 11 mg/L.

The CD spectrum of **1**'s LB films was measured on a Jasco J-820K spectropolarimeter. Ten-layered LB films were transferred onto a CaF_2 disk by a vertical dipping method at a surface pressure of 20 mN/m.

The molar ellipticity [θ] of the peptide LB film was calculated by

$$[\theta] = \frac{\theta A N_A}{nl} \times 10^{-19} \text{ deg cm}^2/\text{dmol}$$

where θ [deg] is the ellipticity; A [nm^2/molecule], the surface area per molecule at a surface pressure of 20 mN/m; n, the total number of amino acid residues in **1** (16); l, the number of LB layers (10); and N_A, Avogadro's constant. CD spectra were recorded at room temperature in a region of 260 to 190 nm, with an integration number of 64.

TM-FTIR spectra of **1**'s LB films were recorded at room temperature on a Perkin-Elmer Spectrum 2000 spectrometer by using a mercury−cadmium−tellurium detector (resolution, 4 cm^{-1}; number of scans, 2048). The LB sample used in the preceding CD measurement was used here. The obtained spectra in the region 1800−1500 cm^{-1} were computationally resolved into individual absorption bands with a Gaussian/Lorentzian (9:1 ratio) function through curve fitting of experimental ones. ^{1}H NMR spectra were recorded on a Bruker DPX-200 spectrometer (200 MHz).

Microscopic Measurements. The particle sizes of Au(Ade-)NPs and Au(C_3)NPs were estimated from AFM observation. An aliquot of a suspended chloroform solution of these nanoparticles was placed on a freshly cleaved mica surface at room temperature in a clean chamber. Each nanoparticle can be fully adsorbed onto the mica surface. Here an excess of the suspended solution on the surface was removed with filter paper. AFM images were observed on a Nano Scope IV instrument (Veeco Instruments) at a scanning speed of 1 Hz for the line frequency by using silicon cantilevers (125 μm in length; 12 nm tip radius).

The morphologies of the peptide template only and of Au nanoparticles adsorbed on the template were observed by AFM measurement. Peptide **1**'s LB monolayers dispersed on an aqueous surface were transferred onto a freshly cleaved mica surface through a vertical dipping method with upstroke at a surface pressure of 10, 15, or 20 mN/m.

Au nanoparticles were adsorbed onto the peptide template prepared at a surface pressure of 20 mN/m. The peptide template was immersed into a chloroform suspension of Au nanoparticles at 20 or 40 °C. After incubation for 1 or 24 h, the template was rinsed with chloroform several times. An amplitude ratio of tip oscillation of 0.8 and higher was used to avoid damaging the sample. All original images were sampled at a resolution of 1024 × 1024 points.

To quantify orientations of the peptide lane and nanoparticle, we used an order parameter P_2, which can be calculated from 2D-FFT of the original AFM image.[38,39] P_2 is derived from

$$P_2 = \frac{3\langle\cos^2\phi\rangle - 1}{2} \quad (-0.5 \le P_2 \le 0)$$

$$\langle\cos^2\phi\rangle = \frac{\int_0^{\pi} d\phi (I_q(\phi)\cdot\cos^2(\phi)\cdot|\sin(\phi)|)}{\int_0^{\pi} d\phi (I_q(\phi)\cdot|\sin(\phi)|)} \quad \left(0 \le \cos^2\phi \le \frac{1}{3}\right)$$

P_2 ranges from −0.5 to 0, where $P_2 = -0.5$ is perfectly oriented. The angle φ quantifies the in-plane direction, with $\varphi = 0°$ corresponding to the direction perpendicular to a slow scan axis of the AFM probe. The size of the AFM image was adjusted to 500 × 500 nm^2 as an efficient size for peptide nanopattern, and the "flatten image processing" was carried out with Nanoscope 6.11.r1 software. The power spectral map was also calculated through 2D-FFT of the AFM image, and the azimuthal angular intensity distributions were plotted on the power spectrum against angle φ ranging from 0° to 180°.

Supporting Information Available: Variable-temperature NMR data of a pair of thyminyl and adenyl compounds; synthetic scheme of peptide **1** and adenine-modified Au particles; ^{1}H NMR spectrum of peptide **1**. This material is available free of charge *via* the Internet at http://pubs.acs.org.

REFERENCES AND NOTES

1. Fersht, A. R. The Hydrogen Bond in Molecular Recognition. *Trends Biochem. Sci.* **1987**, *12*, 301–304.
2. Gygi, S. P.; Rist, B.; Gerber, S. A.; Turecek, F.; Gelb, M. H.; Aebersold, R. Quantitative Analysis of Complex Protein Mixtures Using Isotope-Coded Affinity Tags. *Nature* **1999**, *17*, 994–999.
3. Brust, M.; Bethell, D; Kiely, C. J.; Schiffrin, D. J. Self-Assembled Gold Nanoparticle Thin Films with Nonmetallic Optical and Electronic Properties. *Langmuir* **1998**, *14*, 5425–5429.
4. Sato, T.; Ahmed, H.; Brown, D.; Johnson, B. F. G. Single Electron Transistor Using a Molecularly Linked Gold Colloidal Particle Chain. *J. Appl. Phys.* **1997**, *82*, 696–701.
5. Lopez, N.; Nørskov, J. K. Catalytic CO Oxidation by a Gold Nanoparticle: A Density Functional Study. *J. Am. Chem. Soc.* **2002**, *124*, 11262–11263.
6. Nath, N.; Chilkoti, A. A Colorimetric Gold Nanoparticle Sensor to Interrogate Biomolecular Interactions in Real Time on a Surface. *Anal. Chem.* **2002**, *74*, 504–509.
7. Xue, M.; Zhang, Z.; Zhu, N.; Wang, F.; Zhao, X. S.; Cao, T. Transfer Printing of Metal Nanoparticles with Controllable Dimensions, Placement, and Reproducible Surface-Enhanced Raman Scattering Effects. *Langmuir* **2009**, *25*, 4347–4351.
8. Umetsu, M.; Mizuta, M.; Tsumoto, K.; Ohara, S.; Takami, S.; Watanabe, H.; Kumagai, I.; Adschiri, T. Bioassisted Room-Temperature Immobilization and Mineralization of Zinc Oxide—The Structural Ordering of ZnO Nanoparticles into a Flower-Type Morphology. *Adv. Mater.* **2005**, *17*, 2571–2575.
9. Haginoya, C.; Heike, S.; Ishibashi, M.; Nakamura, K.; Koike, K.; Yoshimura, T.; Yamamoto, J.; Hirayama, Y. Magnetic Nanoparticle Array with Perpendicular Crystal Magnetic Anisotropy. *J. Appl. Phys.* **1999**, *85*, 8327–8331.
10. Chen, C.-L.; Zhang, P.; Rosi, N. L. A New Peptide-Based Method for the Design and Synthesis of Nanoparticle Superstructures: Construction of Highly Ordered Gold Nanoparticle Double Helices. *J. Am. Chem. Soc.* **2008**, *130*, 13555–13557.
11. Chen, C.-L.; Rosi, N. L. Preparation of Unique 1-D Nanoparticle Superstructures and Tailoring Their Structural Features. *J. Am. Chem. Soc.* **2010**, *132*, 6902–6903.
12. Whaley, S. R.; English, D. S.; Hu, E. L.; Barbara, P. F.; Belcher, A. M. Selection of Peptides with Semiconductor Binding Specificity for Directed Nanocrystal Assembly. *Nature* **2000**, *405*, 665–668.
13. Gothelf, K. V.; LaBean, T. H. DNA-Programmed Assembly of Nanostructures. *Org. Biomol. Chem.* **2005**, *3*, 4023–4037.
14. Bitton, R.; Schmidt, J.; Biesalski, M.; Tu, R.; Tirrell, M.; Bianco-Peled, H. Self-Assembly of Model DNA-Binding Peptide Amphiphiles. *Langmuir* **2005**, *21*, 11888–11895.
15. Lalander, C. H.; Zheng, Y.; Dhuey, S.; Cabrini, S.; Bach, U. DNA-Directed Self-Assembly of Gold Nanoparticles onto Nanopatterned Surfaces: Controlled Placement of Individual Nanoparticles into Regular Arrays. *ACS Nano* **2010**, *4*, 6153–6161.
16. Burkoth, T. S.; Benzinger, T. L. S.; Jones, D. N. M.; Hallenga, K.; Meredith, S. C.; Lynn, D. G. C-Terminal PEG Blocks the Irreversible Step in β-Amyloid(10−35) Fibrillogenesis. *J. Am. Chem. Soc.* **1998**, *120*, 7655–7656.
17. Zhang, S.; Holmes, T.; Lockshin, C.; Rich, A. Spontaneous Assembly of a Self-Complementary Oligopeptide to Form a Stable Macroscopic Membrane. *Proc. Natl. Acad. Sci.* **1993**, *90*, 3334–3338.
18. Fukushima, Y. Alcohol-Induced Helix-Sheet Transition of a Sequential Alternating Amphiphilic Polypeptide. *Chem. Lett.* **1999**, *2*, 157–158.
19. Sugimoto, N.; Zou, J.; Kazuta, H.; Miyoshi, D. $\alpha-\beta$ Structural Transition of Short Oligopeptides by Water/Organic Solvent Titration. *Chem. Lett.* **1999**, *7*, 637–638.
20. Koga, T.; Taguchi, K.; Kobuke, Y.; Kinoshita, T.; Higuchi, M. Structural Regulation of a Peptide-Conjugated Graft Copolymer: A Simple Model for Amyloid Formation. *Chem.—Eur. J.* **2003**, *9*, 1146–1156.
21. Fung, S. Y.; Keyes, C.; Duhamel, J.; Chen, P. Concentration Effect on the Aggregation of a Self-Assembling Oligopeptide. *Biophys. J.* **2003**, *85*, 537–548.
22. Greenfield., N.; Fasman, G. D. Computed Circular Dichroism Spectra for the Evaluation of Protein Conformation. *Biochemistry* **1969**, *8*, 4108–4116.
23. Miyazawa, T.; Blout, E, R. The Infrared Spectra of Polypeptides in Various Conformations: Amide I and II Bands. *J. Am. Chem. Soc.* **1961**, *83*, 712–719.
24. Winningham, M. J.; Sogah, D. Y. A Modular Approach to Polymer Architecture Control via Catenation of Prefabricated Biomolecular Segments: Polymers Containing Parallel β-Sheets Templated by a Phenoxathiin-Based Reverse Turn Mimic. *Macromolecules* **1997**, *30*, 862–876.
25. Higuchi, M.; Inoue, T.; Miyoshi, H.; Kawaguchi, M. pH-Induced Reversible Conformational and Morphological Regulation of Polyleucine Grafted Polyallylamine Assembly in Solution. *Langmuir* **2005**, *21*, 11462–11467.
26. Toniolo, C.; Palumbo, M. Solid-State Infrared Absorption Spectra and Chain Arrangement in Some Synthetic Homo-oligopeptides in the Intermolecularly Hydrogen-Bonded

Pleated-Sheet β-Conformation. *Biopolymers* **1977**, *16*, 219–224.
27. Shimmin, R. G.; Schoch, A. B.; Braun, P. V. Polymer Size and Concentration Effects on the Size of Gold Nanoparticles Capped by Polymeric Thiols. *Langmuir* **2004**, *20*, 5613–5620.
28. Balcome, S.; Park, S.; Dorr, D. R. Q.; Hafner, L.; Phillips, L.; Tretyakova, N. Adenine-Containing DNA−DNA Cross-Links of Antitumor Nitrogen Mustards. *Chem. Res. Toxicol.* **2004**, *17*, 950–952.
29. Higuchi, M.; Ushida, K.; Kawaguchi, M. Structural Control of Peptide-Coated Gold Nanoparticle Assemblies by the Conformational Transition of Surface Peptides. *J. Colloid Interface Sci.* **2007**, *308*, 356–363.
30. Adenine (A) and thymine (T) are hydrogen-bonded not only with Watson−Crick base pairing but also in three additional manners (reverse Watson−Crick, Hoogsteen, and reversed Hoogsteen base pairing).[31,32] One of the four possible manners is not identified in the present system, whereas standard Watson−Crick base pairing is depicted in Figure 1 and the table of contents graphic. Whatever the pairing types are, the formation of A−T diads does not change the 2D pattern of Au nanoassembly. Triads such as A−A−T and T−A−T might be formed to influence the original Au-assembly pattern. However, the formation of such triad species might be energetically disfavored due to steric reasons.
31. Kool, E. T. Circular Oligonucleotides: New Concepts in Oligonucleotide Design. *Annu. Rev. Biophys. Biomol. Struct.* **1996**, *25*, 1–28.
32. Cheng, Y.-K.; Pettitt, B. M. Hoogsteen versus Reversed-Hoogsteen Base Pairing: DNA Triple Helices. *J. Am. Chem. Soc.* **1992**, *114*, 4465–4474.
33. Fields, G. B.; Noble, R. L. Solid Phase Peptide Synthesis Utilizing 9-Fluorenylmethoxycarbonyl Amino Acids. *Int. J. Pept. Protein Res.* **1990**, *35*, 161–214.
34. Aletras, A.; Barlos, K.; Gatos, D.; Koutsogianni, S.; Mamos, P. Preparation of the Very Acid-Sensitive Fmoc-Lys(Mtt)-OH Application in the Synthesis of Side-Chain to Side-Chain Cyclic Peptides and Oligolysine Cores Suitable for the Solid-Phase Assembly of MAPs and TASPs. *Int. J. Pept. Protein Res.* **1995**, *45*, 488–496.
35. Hancock, W. S.; Battersby, J. E. A New Micro-Test for the Detection of Incomplete Coupling Reactions in Solid-Phase Peptide Synthesis Using 2,4,6-Trinitrobenzene-Sulphonic Acid. *Anal. Biochem.* **1976**, *71*, 260–264.
36. Brust, M.; Walker, M.; Bethell, D.; Schiffrin, D. J.; Whyman, R. Synthesis of Thiol-Derivatised Gold Nanoparticles in a Two-Phase Liquid−Liquid System. *J. Chem. Soc., Chem. Commun.* **1994**, *7*, 801–802.
37. Caruthers, M. H.; Barone, A. D.; Beaucage, S. L.; Dodds, D. R.; Fisher, E. F.; McBride, L. J.; Matteucci, M.; Stabinsky, Z.; Tang, J. -Y. Chemical Synthesis of Deoxyoligonucleotides by the Phosphoramidite Method. *Methods Enzymol.* **1987**, *154*, 287–313.
38. Olszowka, V.; Hund, M.; Kuntermann, V.; Scherdel, S.; Tsarkova, L.; Böker, A.; Kraush, G. Large Scale Alignment of a Lamellar Block Copolymer Thin Film via Electric Fields: a Time-Resolved SFM Study. *Soft Matter* **2006**, *2*, 1089–1094.
39. Olszowka, V.; Kuntermann, V.; Böker, A. Control of Orientational Order in Block Copolymer Thin Films by Electric Fields: A Combinatorial Approach. *Macromolecules* **2008**, *41*, 5515–5518.